Exploration of immunoglobulin transcriptomes from mice immunized with three-finger toxins and phospholipases A$_2$ from the Central American coral snake, *Micrurus nigrocinctus*

Andreas H Laustsen [Corresp., 1] , **Mikael Engmark** [1, 2] , **Christopher Clouser** [3, 4] , **Sonia Timberlake** [5] , **Francois Vigneault** [3, 4] , **José María Gutiérrez** [6] , **Bruno Lomonte** [6]

[1] Department of Biotechnology and Biomedicine, Technical University of Denmark, Kgs. Lyngby, Denmark

[2] Department of Bio and Health Informatics, Technical University of Denmark, Kgs. Lyngby, Denmark

[3] Juno Therapeutics, Seattle, Washington, United States of America

[4] AbVitro, Boston, Massachusetts, United States of America

[5] Finch Therapeutics, Somerville, Massachusetts, United States of America

[6] Instituto Clodomiro Picado, Universidad de Costa Rica, San José, Costa Rica

Corresponding Author: Andreas H Laustsen
Email address: ahola@bio.dtu.dk

Snakebite envenomings represent a neglected public health issue in many parts of the rural tropical world. Animal-derived antivenoms have existed for more than a hundred years and are effective in neutralizing snake venom toxins when timely administered. However, the low immunogenicity of many small but potent snake venom toxins represents a challenge for obtaining a balanced immune response against the medically relevant components of the venom. Here, we employ high-throughput sequencing of the immunoglobulin (Ig) transcriptome of mice immunized with a three-finger toxin and a phospholipase A$_2$ from the venom of the Central American coral snake, *Micrurus nigrocinctus.* Although exploratory in nature, our indicate results showed that only low frequencies of mRNA encoding IgG isotypes, the most relevant isotype for therapeutic purposes, were present in splenocytes of five mice immunized with 6 doses of the two types of toxins over 90 days. Furthermore, analysis of Ig heavy chain transcripts showed that no particular combination of variable (V) and joining (J) gene segments had been selected in the immunization process, as would be expected after a strong humoral immune response to a single antigen. Combined with the titration of toxin-specific antibodies in the sera of immunized mice, these data support the low immunogenicity of three-finger toxins and phospholipases A$_2$ found in *M. nigrocinctus* venoms, and highlight the need for future studies analyzing the complexity of antibody responses to toxins at the molecular level.

1   Exploration of immunoglobulin transcriptomes from mice immunized with three-

2   finger toxins and phospholipases A$_2$ from the Central American coral snake,

3   *Micrurus nigrocinctus*

5   Andreas H. Laustsen[1*], Mikael Engmark[1,2], Christopher Clouser[3,4], Sonia Timberlake[5], Francois

6   Vigneault[3,4], José María Gutiérrez[6], Bruno Lomonte[6]

8   [1] Department of Biotechnology and Biomedicine, Technical University of Denmark, Denmark
9   [2] Department of Bio and Health Informatics, Technical University of Denmark, Denmark
10   [3] Juno Therapeutics, Seattle (WA), USA
11   [4] AbVitro, Boston (MA),USA
12   [5] Finch Therapeutics, Somerville (MA), USA
13   [6] Instituto Clodomiro Picado, Facultad de Microbiología, Universidad de Costa Rica,
14   San José, Costa Rica

16   **Running title**: Antibody isotyping of immune response against coral snake toxins

19   [*] **Address correspondence to**:
20
21   Dr. Andreas H. Laustsen (ahola@bio.dtu.dk), Department of Biotechnology and Biomedicine,

22   Technical University of Denmark, Denmark

Abstract

Snakebite envenomings represent a neglected public health issue in many parts of the rural tropical world. Animal-derived antivenoms have existed for more than a hundred years and are effective in neutralizing snake venom toxins when timely administered. However, the low immunogenicity of many small but potent snake venom toxins represents a challenge for obtaining a balanced immune response against the medically relevant components of the venom. Here, we employ high-throughput sequencing of the immunoglobulin (Ig) transcriptome of mice immunized with a three-finger toxin and a phospholipase A_2 from the venom of the Central American coral snake, *Micrurus nigrocinctus*. Although exploratory in nature, our indicate results showed that only low frequencies of mRNA encoding IgG isotypes, the most relevant isotype for therapeutic purposes, were present in splenocytes of five mice immunized with 6 doses of the two types of toxins over 90 days. Furthermore, analysis of Ig heavy chain transcripts showed that no particular combination of variable (V) and joining (J) gene segments had been selected in the immunization process, as would be expected after a strong humoral immune response to a single antigen. Combined with the titration of toxin-specific antibodies in the sera of immunized mice, these data support the low immunogenicity of three-finger toxins and phospholipases A_2 found in *M. nigrocinctus* venoms, and highlight the need for future studies analyzing the complexity of antibody responses to toxins at the molecular level.

(232 words)

1. Introduction

Snakebite envenomings represent a major public health concern in tropical regions of the world (*Williams et al., 2011*). Despite emerging discoveries that may one day pave the way for novel biotechnology-based antivenoms (reviewed by *Laustsen et al., 2016a*; *2016b*), animal serum-derived antivenoms remain the cornerstone of snakebite envenoming treatment (*Gutiérrez et al., 2011*). Production of antivenom is challenged by a large variation in immunogenicity of many key snake venom toxins resulting in unpredictable immune responses in production animals (*Cook et al., 2010*; *Guidolin et al., 2010*). It has been shown that many of the immunogenic venom components are in fact not important for toxicity (*Antúnez et al., 2010*; *Gutiérrez et al., 2009; Laustsen et al., 2015*), and conversely, that some highly toxic venom components, such as α-neurotoxins (both short and long neurotoxins), phospholipases A_2, and P-I snake venom metalloproteinases may be poorly immunogenic (*Schottler, 1951*; *Gutiérrez et al., 2009*; *Chotwiwatthanakun et al., 2001*; *Ownby & Colberg, 1990*; *Judge et al., 2006; Wong et al., 2016; Tan et al., 2016; Leong et al., 2015; Tan et al., 2015*). Combined, this creates a challenge for antivenom production, since the goal of obtaining an antivenom with a strong, yet balanced response against all the medically relevant toxins becomes a complex endeavor.

Coral snakes (genera *Micrurus*, *Leptomicrurus*, and *Micruroides*) are, together with the sea snake *Hydrophis* (*Pelamis*) *platura*, the representatives of the snake family Elapidae in the Americas, comprising approximately 85 species (*Campbell & Lamar, 2004*; the Reptile Database - www.reptile-database.org). Although *Micrurus* species are only responsible for about 1-2% of snakebite cases in this continent, roughly corresponding to 750 to 1000 cases per year, envenomings by these snakes can be fatal if not treated properly and timely (*Warrell, 2004; Gutiérrez, 2014; Bucaretchi et al., 2016*). Envenomings resulting from coral snakebites are

67 predominantly associated with descending neuromuscular paralysis, which may end in

68 respiratory arrest (*Warrell, 2004; Bucaretchi et al., 2016*).

69   Production of antivenoms against *Micrurus* snakes is particularly challenging, as (a) it is

70 very difficult to maintain coral snakes in captivity (Chacón et al., 2012); (b) the majority of

71 *Micrurus* species provide a very low yield of venom, implying that the collection of the

72 quantities of venom required for horse immunization and quality control testing demands the

73 'milking' of many specimens (Chacón et al., 2012; Bolaños, 1972); and (c) there is a variable

74 extent of immunological cross-recognition between venoms from coral snakes of different

75 species; hence, antivenoms raised against some species are not always effective in the

76 neutralization of venoms of other species (*Bolaños, Cerdas & Abalos, 1978; Tanaka et al.,*

77 *2016*). As a result, only a few laboratories manufacture *Micrurus* antivenoms, and several

78 countries where these snakes inhabit completely lack this therapeutic resource, e.g. Venezuela,

79 Ecuador, Peru, Bolivia, the Guyanas, and Paraguay, which severely limits the clinical

80 management of these accidents.

81   Knowledge on the composition of the venoms of *Micrurus* species has increased steadily

82 over the last years, as a consequence of proteomic characterizations (reviewed by *Lomonte et al.,*

83 *2016b*). Two main venom phenotype patterns have been identified, i.e. venoms rich in

84 neurotoxins of the three-finger toxin (3FTx) family, and venoms rich in phospholipases A_2

85 (PLA_2s) (*Fernández et al., 2015*). In addition to these two main protein families, other minor

86 components of these venoms include L-amino acid oxidases, serine proteinases,

87 metalloproteinases, nerve growth factor, C-type lectin-like proteins, Kunitz-type inhibitors,

88 among others (*Fernández et al., 2011, 2015; Corrêa-Netto et al., 2011; Lomonte et al., 2016a;*

89 *Sanz et al., 2016; Rey-Suárez et al., 2011, 2016*). In some cases, the toxins playing the main role

90   in overall toxicity have been identified, these being 3FTxs and PLA$_2$s (*Rey-Suárez et al., 2012;*

91   *Vergara et al., 2014*; *Fernández et al., 2015; Castro et al., 2015; Ramos et al., 2016*).

92   The limited immunogenicity of the highly toxic PLA$_2$s and 3FTxs (*Fernández et al.,*

93   *2011*, *Rosso et al., 1996*; *Alape-Girón et al., 1996*) represents another difficulty in production of

94   *Micrurus* antivenom, since it thwarts the goal of raising a balanced immune response against

95   these medically relevant toxins. In order to further explore how these toxins interact with the

96   mammalian immune system, we chose a mouse model and employed an NGS approach using the

97   AbSeq™   technology   developed   by   AbVitro   (now   Juno   Therapeutics,

98   https://www.junotherapeutics.com), based on Illumina sequencing (Fig. 1). The methodology

99   was utilized to sequence immunoglobulin (Ig) encoding mRNA transcripts from splenic B-

100 lymphocytes in mice subjected to immunization with either a 3FTx or a PLA$_2$ toxin from the

101 venom of *M. nigrocinctus* (Central American coral snake). By this approach, the transcription

102 levels of different immunoglobulin isotypes and dominant clones of B-lymphocytes with a

103 particular usage of V (variable) and J (joining) gene segments can be determined for Ig heavy

104 chain transcripts. This methodology has previously been employed for investigating B-cell

105 populations in autoimmune (*Stern et al., 2014*) or infectious diseases (*Tsioris et al., 2015*; *Di*

106 *Niro et al., 2015*), for example. By employing the AbSeq™ high-throughput approach, we

107 explore, for the first time, the Ig transcriptome including VJ usage patterns in individual animals

108 subjected to immunization with two relevant toxin classes of elapid snakes. Although

109 exploratory in its nature and somewhat limited by a small sample size, this study thus provides

110 novel insight into the humoral response of mice immunized with 3FTx or PLA$_2$ toxins and

111 highlights important challenges of raising antibodies against poorly immunogenic toxins.

112

113
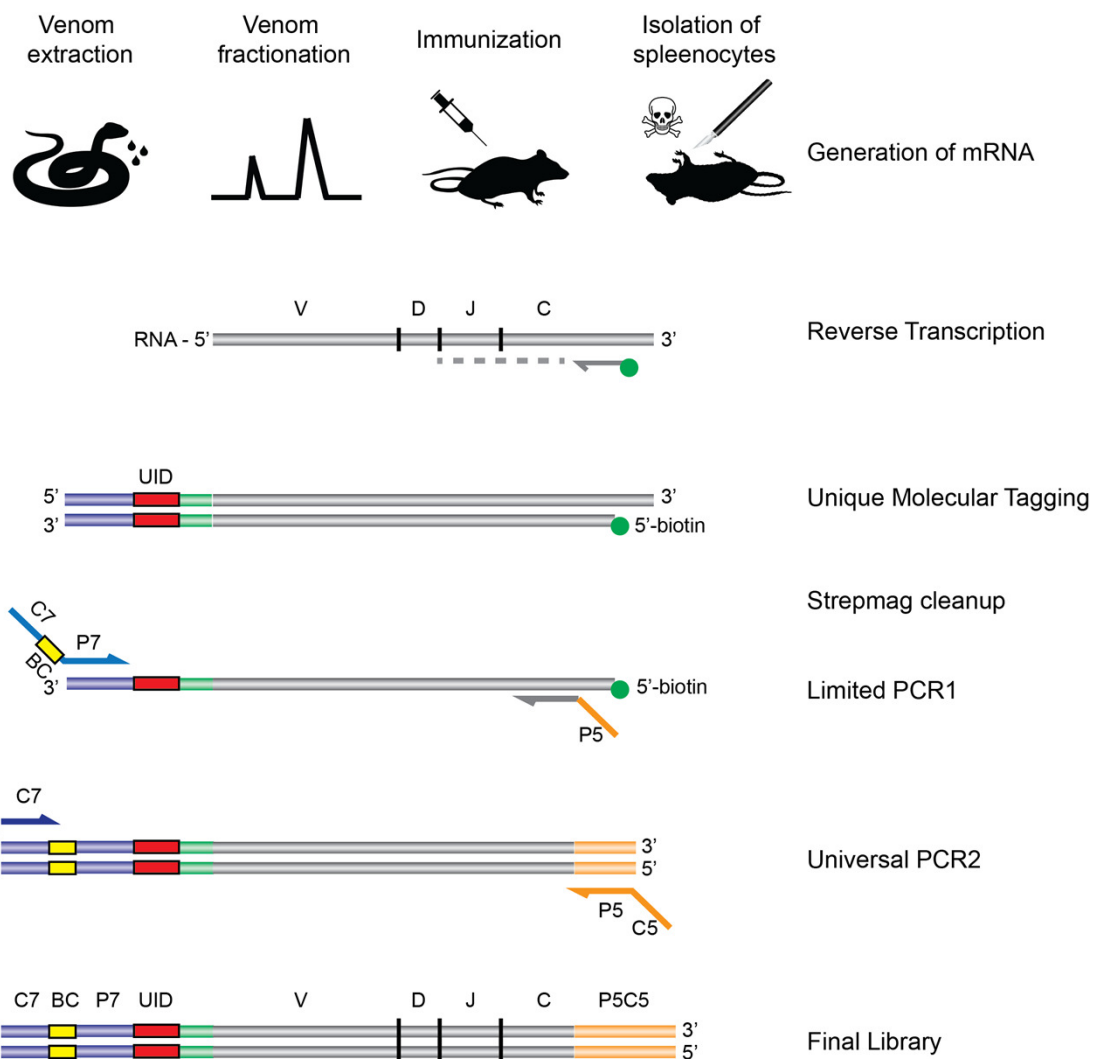
Figure 1: *Schematic overview of the experimental strategy. Following extraction from the snakes, venom is fractionated by HPLC, and the fractions of interest are used for immunization of rodents. Upon completion of the immunization protocol, the rodents are sacrificed and RNA is extracted and subjected to the AbSeq protocol (see Materials and Methods), whereby the RNA is reverse transcribed and barcoded, allowing for correct pairing of V_H and V_L chains after DNA sequencing.*

120

121 **2. Materials and Methods**

122 *2.1 Snake venom and toxins*

123   Venom from *M. nigrocinctus* was obtained from a pool of more than 50 adult specimens

124   collected in the Central Pacific region of Costa Rica, kept at the serpentarium of Instituto

125   Clodomiro Picado, Universidad de Costa Rica. The snakes were not collected for this study, but

126   belong to Instituto Clodomiro Picado, where their venoms are routinely used for the production

127   of antivenom, wherefore a field permit was not necessary. Venom extraction is performed every

128   four months (Chacón et al., 2012). The venom was lyophilized and stored at -20°C.

129   Fractionation of the venom was performed by RP-HPLC on a C_{18} column (4.6 x 250 mm, 5

130   µm particle diameter; Supelco) as previously described (*Fernández et al., 2011*). In brief, 2 mg

131   of venom dissolved in 200 µL of water containing 0.1% trifluoroacetic acid (TFA; solution A)

132   were separated at 1 mL/min in an Agilent 1200 chromatograph monitored at 215 nm, applying a

133   gradient towards solution B (acetonitrile, containing 0.1% TFA): 0% B for 5 min, 0–15% B over

134   10 min, 15–45% B over 60 min, 45–70% B over 10 min, and 70% B over 9 min. Fractions of

135   interest (the major components of the venom, belonging to the 3FTx (lethal) and PLA_2

136   (myotoxic) protein families) were collected manually, dried in a vacuum centrifuge, and

137   identified by trypsin digestion followed by MALDI-TOF/TOF mass spectrometry (*Fernández et*

138   *al., 2011*). Proteins were redissolved in water and their concentrations were estimated on the

139   basis of their absorbance at 280 nm, using a NanoDrop (Thermo) instrument.

140

141   *2.2 Immunization of mice*

142   Three female CD-1 mice (16-18 g) from Instituto Clodomiro Picado were immunized with a

143   three-finger toxin (3FTx), and two with a phospholipase A_2 (PLA_2), respectively. These

144   correspond to fractions #3 (~P80548) and #30 (~P81166/P81167) described in the previous

145   proteomic characterization of this venom (*Fernández et al., 2011*). All toxin doses were injected

146 by the intraperitoneal route. The priming dose was 1 µg emulsified in Freund's complete

147 adjuvant, followed by five booster doses injected in physiological saline without adjuvant, at

148 days 15 (1 µg), 43 (2 µg) 63 (4 µg), and 83 (6 µg for the 3FTx and 8 µg for the PLA_2). At day

149 90, after obtaining a blood sample for monitoring of the antibody response by enzyme-

150 immunoassay, mice were euthanized by CO_2 inhalation. Their spleens were immediately

151 removed, cut in small pieces, and disaggregated over a stainless steel mesh to obtain splenocytes.

152 These cell suspensions were aliquoted in RNAlater® solution (Thermo) and shipped within 24 h

153 to AbVitro, at room temperature, for subsequent molecular studies. The use of animals for these

154 experiments followed the ethical guidelines of the *Comité Institucional para el Uso y Cuido de*

155 *Animales* (CICUA), Universidad de Costa Rica, with the approval number 82-08.

156

157 *2.3 Enzyme-immunoassay (ELISA)*

158 In order to evaluate the individual antibody responses of the mice, wells in MaxiSorp 96-well

159 plates (NUNC, Roskilde, Denmark) were coated overnight with 1 µg of either 3FTx or PLA_2,

160 dissolved in 100 µL PBS (0.12 M NaCl, 0.04 M sodium phosphate, pH 7.2). Wells were washed

161 five times with PBS and blocked by adding 100 µL PBS containing 2% (w:v) bovine serum

162 albumin (BSA, Sigma), and incubated at room temperature for 1 h. Plates were then washed five

163 times with PBS. Serial dilutions of serum from each mouse were prepared in PBS + 2% BSA

164 and 100 µL was added to each well, in triplicates, and incubated overnight at 4°C. Normal mouse

165 serum, run simultaneously under identical conditions was used as a control for background.

166 Plates were then washed five times with PBS, followed by the addition of 100 µL of a 1:3000

167 dilution of anti-mouse IgG (whole molecule) antibodies conjugated to alkaline phosphatase, in

168 PBS + 1% BSA. The plates were incubated for 2 h, and then washed five times with FALC

169 buffer (0.05 M Tris, 0.15 M NaCl, 20 µM ZnCl$_2$, 1 mM MgCl$_2$, pH 7.4). Development of color

170 was attained by addition of 100 µL p-nitrophenyl phosphate (1 mg/mL in 9.7% v/v

171 diethanolamine buffer, pH 9.8) and absorbances at 405 nm were recorded (Multiskan FC,

172 Thermo Scientific).

173

174 *2.4 Assessment of mRNA quality*

175 Assessment of RNA quality was performed using Agilent's TapeStation according to the

176 manufacturers protocol and algorithm to calculate RIN^e scores

177 (http://www.agilent.com/cs/library/technicaloverviews/public/5990-9613EN.pdf).

178

179 *2.5 Library preparation and high-throughput sequencing of B-cell receptors*

180 The method for high-throughput sequencing of the B-cell repertoire was performed as described

181 elsewhere (*Di Niro et al., 2015*; *Tsioris et al., 2015*). Briefly, RNA was reverse-transcribed into

182 cDNA using a biotinylated oligo dT primer. An adaptor sequence was added to the 3' end of all

183 cDNA, which contains the Illumina P7 universal priming site and a 17-nucleotide unique

184 molecular identifier (UMI). Products were purified using streptavidin-coated magnetic beads

185 followed by a primary PCR reaction using a pool of primers targeting the IGHA, IGHD, IGHE,

186 IGHG, IGHM, IGKC and IGLC regions, as well as a sample-indexed Illumina P7C7 primer. The

187 immunoglobulin-specific primers contained tails corresponding to the Illumina P5 sequence.

188 PCR products were then purified using AMPure XP beads. A secondary PCR was then

189 performed to add the Illumina C5 clustering sequence to the end of the molecule containing the

190 constant region. The number of secondary PCR cycles was tailored to each sample to avoid

191 entering plateau phase, as judged by a prior quantitative PCR analysis. The final products

192   (reverse-transcribed UTR + VDJ + partial - Cexon segments of the transcripts of the

193   immunoglobulin chains, plus molecular barcode, Illumina multiplexing barcode, and Illumina

194   sequencing adapters) were purified, quantified with Agilent TapeStation and pooled in equimolar

195   proportions, followed by high-throughput paired-end sequencing on the Illumina MiSeq

196   platform. For sequencing, the Illumina 600 cycle kit was used with the modifications that 325

197   cycles was used for read 1, 6 cycles for the index reads, 300 cycles for read 2 and a 10% PhiX

198   spike-in to increase sequence diversity.

199

200   *2.6 VJ repertoire sequencing data analysis*

201   MiSeq reads were demultiplexed using Illumina software, and processed with the pRESTO

202   toolsuite (*Vander Heiden et al., 2014*) as following: Positions with less than Phred quality 5 were

203   masked with Ns. Isotype-specific primers and molecular barcodes (UIDs or UMIs) were

204   identified in the amplicon and trimmed, using pRESTO MaskPrimers-cut. A read 1 and read 2

205   consensus sequence was generated separately for each mRNA from reads grouped by unique

206   molecular identifier, which are PCR replicates arising from the same original mRNA molecule of

207   origin. UMI read groups were aligned with MUSCLE (*Edgar, 2004*), and pRESTO was used to

208   BuildConsensus, requiring ≥60% of called PCR primer sequences agree for the read group,

209   maximum nucleotide diversity of 0.1, using majority rule on indel positions, and masking

210   alignment columns with low posterior (consensus) quality. Paired end consensus sequences were

211   then stitched in two rounds. First, ungapped alignment of each read pair's consensus sequence

212   termini was optimized using a Z-score approximation and scored with a binomial *p*-value as

213   implemented in pRESTO AssemblePairs-align. For read pairs failing to stitch this way, stitching

214   was attempted using the human BCR germline V exons to scaffold each read prior to stitching or

215   gapped read-joining, using pRESTO's AssemblePairs-reference. Positions with posterior

216   consensus quality less than Phred 5 were masked again with Ns. Each mRNA was annotated for

217   V, D, J germline gene of origin, productivity, and CDR3 region using igblastn (*Ye et al, 2013*).

218   Igblast output was parsed and analyzed with custom scripts as described below (proprietary to

219   AbVitro (now Juno Therapeutics)) and visualized with R (*R Core Team, 2014*). Briefly, clones

220   were defined using a conservative approach, grouping mRNAs from the same V and J germline

221   gene of origin and having the same isotype and CDR3 nucleotide sequence. Non-productive

222   rearrangements (as predicted by Igblast) were excluded from the analysis. Within each sample,

223   clones were ranked by abundance (mRNAs/clone) and plotted to highlight the most expanded

224   binding motifs. To examine preferences for V-J usage common across mice exposed to the same

225   toxin, clones were grouped into larger bins that each encompass a single V gene-J gene

226   combination, but all isotypes and CDR3s.

227

228   *2.7 In silico epitope predictions*

229   The sequences of selected toxin components in the two venom fractions used for immunization

230   were obtained from the UniProtKB database (http://www.uniprot.org) and linear parts of B-cell

231   epitopes were predicted using the Bepi-Pred 1.0 server (*Larsen et al., 2006*) using 0.9 as

232   Threshold to obtain a sensitivity of 0.25 and Specificity of 0.91. As no experimental structures

233   were available, homology models were build based CPHmodels 3.2 (*Nielsen et al., 2010*) and the

234   pdb-files were submitted to DiscoTope 2.0 (*Kringelum et al., 2012*) using 0.5 as Threshold to

235   obtain a sensitivity of 0.23 and Specificity of 0.90.

236

237   **3. Results and Discussion**

238   Three-finger toxins (3FTx) and phospholipase A_2s (PLA_2) are the two most abundant toxin

239   families in the venom of *M. nigrocinctus* (*Fernández et al., 2011*), and generally they are the two

240   snake toxin families which have been most investigated (*Laustsen et al., 2016a*). In the venom of

241   *M. nigrocinctus* these toxins cause neuromuscular paralysis, owing to a combination of pre- and

242   post-synaptic actions, and myotoxicity, providing the venom with its high toxicity (*Rosso et al.,*

243   *1996*; *Alape-Girón et al., 1996*). In previous studies it was observed that 3FTxs and PLA_2s were

244   recognized more weakly than larger proteins from this venom, by a therapeutic equine antivenom

245   (*Fernández et al., 2011*). Despite their low immunogenicity, it was possible to raise an antibody

246   response against both toxins in four out of five mice, although high variation in the antibody titer

247   was observed (Fig. 2). Mice immunized with PLA_2 had a higher antibody titer than mice

248   immunized with the 3FTx, in agreement with the higher molecular mass of the former.

249

250
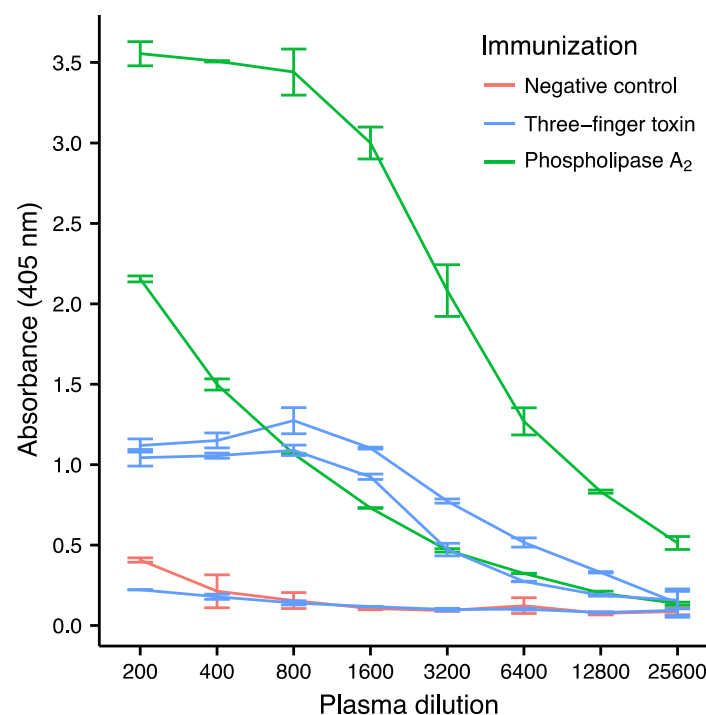
251   ***Figure 2:*** *ELISA titrations of serum antibodies against* M. nigrocinctus *PLA₂ or 3FTx in mice*

252   *following a 90-day immunization protocol. Two mice were immunized with PLA₂, and three were*

253   *immunized with 3FTx. Plates were coated with either PLA₂ or 3FTx, and antibodies were*

254   *detected as described in Materials and Methods.*

255

256   Assessment of the mRNA from harvested mouse splenocytes indicated that it was of sufficient

257   quality to proceed to sequencing (RIN[e] scores between 5.2 and 6.4). A high-throughput

258   sequencing approach (AbSeq™) was employed to investigate transcription levels of Ig isotypes

259   and the usage of V and J gene segments for heavy chain assembly in mice that were immunized

260   with a 3FTx or a PLA₂. Investigation of the 50 most frequent VJ combinations for the

261   immunized mice did not, however, result in identification of a dominant combination, as the VJ

262   usage was found to be similar across all samples (Fig. 3). This finding suggests that the

263   generated antibody responses might be diverse and that multiple specific antibodies with low

264   abundance are generated in each mouse.

265
266
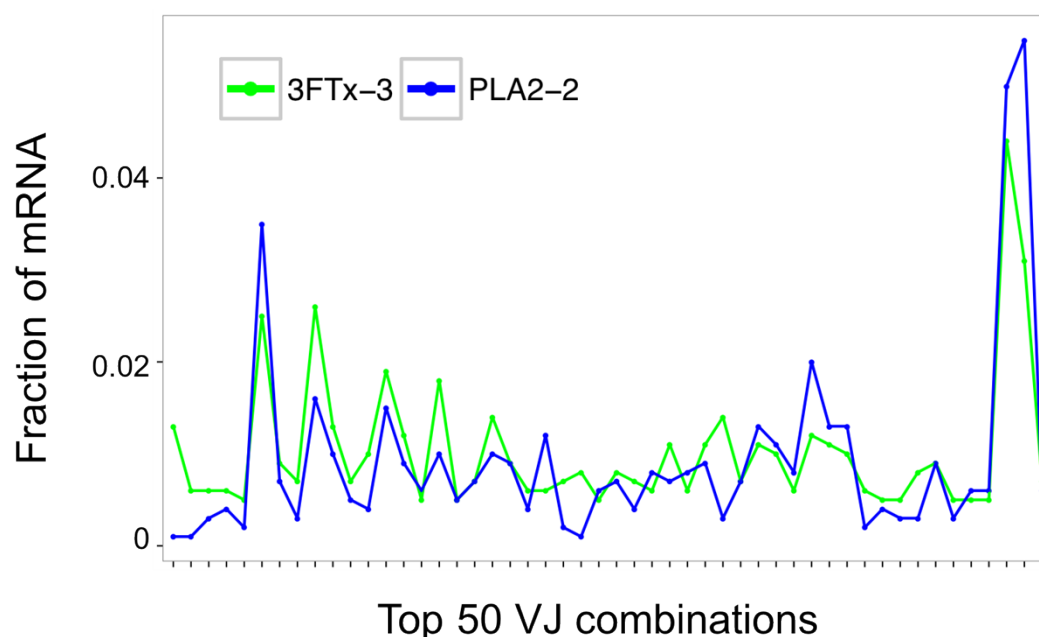
267   *Figure 3. Comparison of the relative abundance of mRNA for the 50 most abundant VJ*

268   *combinations for the mouse 3FTx-3 and mouse PLA_2-2 showing VJ usage to be similar across*

269   *samples. Similar VJ usage patterns were observed for other pairs of immunized mice.*

270

271   Looking at the sequences of all mRNA transcripts encoding heavy chain variable domain (V_H)

272   clones across each sample, we were able to find shared V_H clones with similar relative

273   abundances in either the PLA_2-immunized or the 3FTx-immunized mice (Fig. 4). In comparison,

274   almost no V_H clones were shared between mice immunized with different toxins (Fig. 5). This

275   implies that the immunization procedure did indeed elicit specific, but different responses

276   dependent on whether PLA_2s or 3FTxs were employed for immunization. The relatively high

277   number of V_H clones found in both of the PLA_2-immunized mice (Fig. 4A) compared to lower

278   number of V_H clones found across the three 3FTx-immunized mice (Fig. 4B-D) further indicate

279   that immunization with PLA_2s is more prone to give rise to antibodies transcribed in similar

280   quantities. Also, an intermediate number of similar V_H clones was found in both the PLA_2-1 and

281   3FTx-3 samples (Fig. 5E), even though the correlation in relative abundance was not equally

282   pronounced. This is likely explained by the fact that the majority of V_H clones found in both

283   PLA_2-immunized mice are not expected to be specific towards the toxins, but instead are likely to

284   be directed against other (environmental) antigens that the mice have encountered throughout

285   their life.

286

287
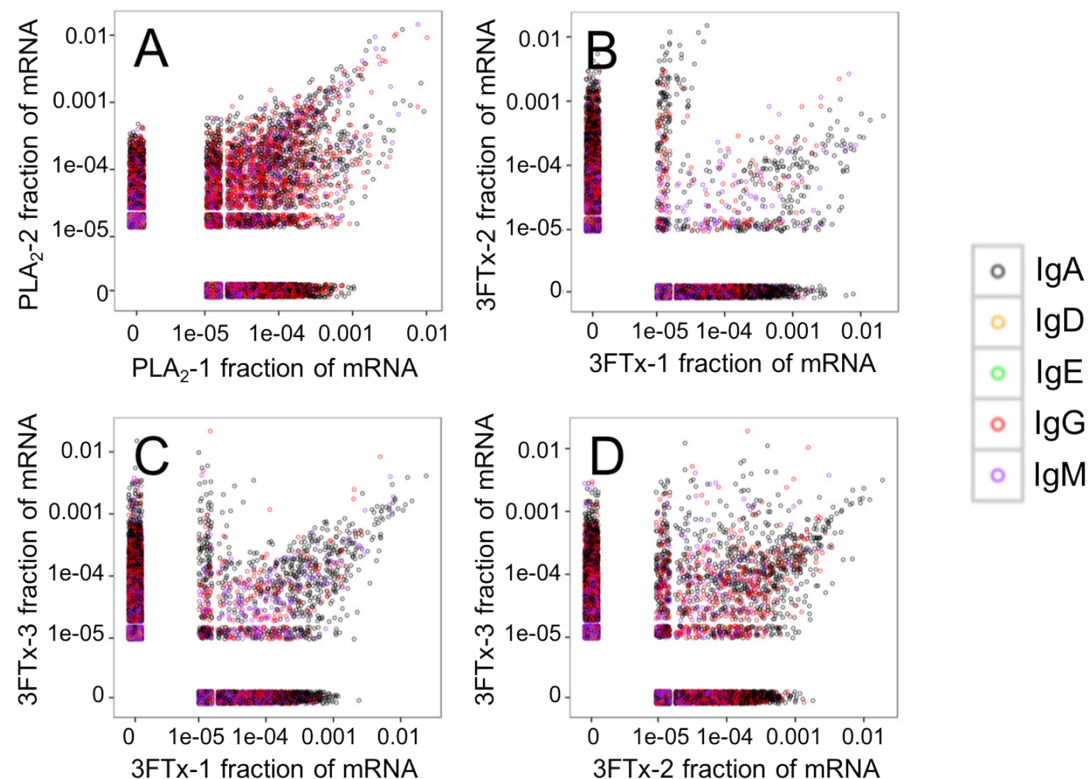
Figure 4: *Relative abundance of unique V_H clone transcripts compared between samples. A*

large group of V_H transcripts are found in similar abundance in different mice immunized with

the same toxin. **A)** *Comparison between mouse PLA$_2$-1 and PLA$_2$-2,* **B)** *Comparison between*

mouse 3FTx-1 and 3FTx-2, **C)** *Comparison between mouse 3FTx-1 and 3FTx-3,* **D)** *Comparison*

between mouse 3FTx-2 and 3FTx-3.

293

294
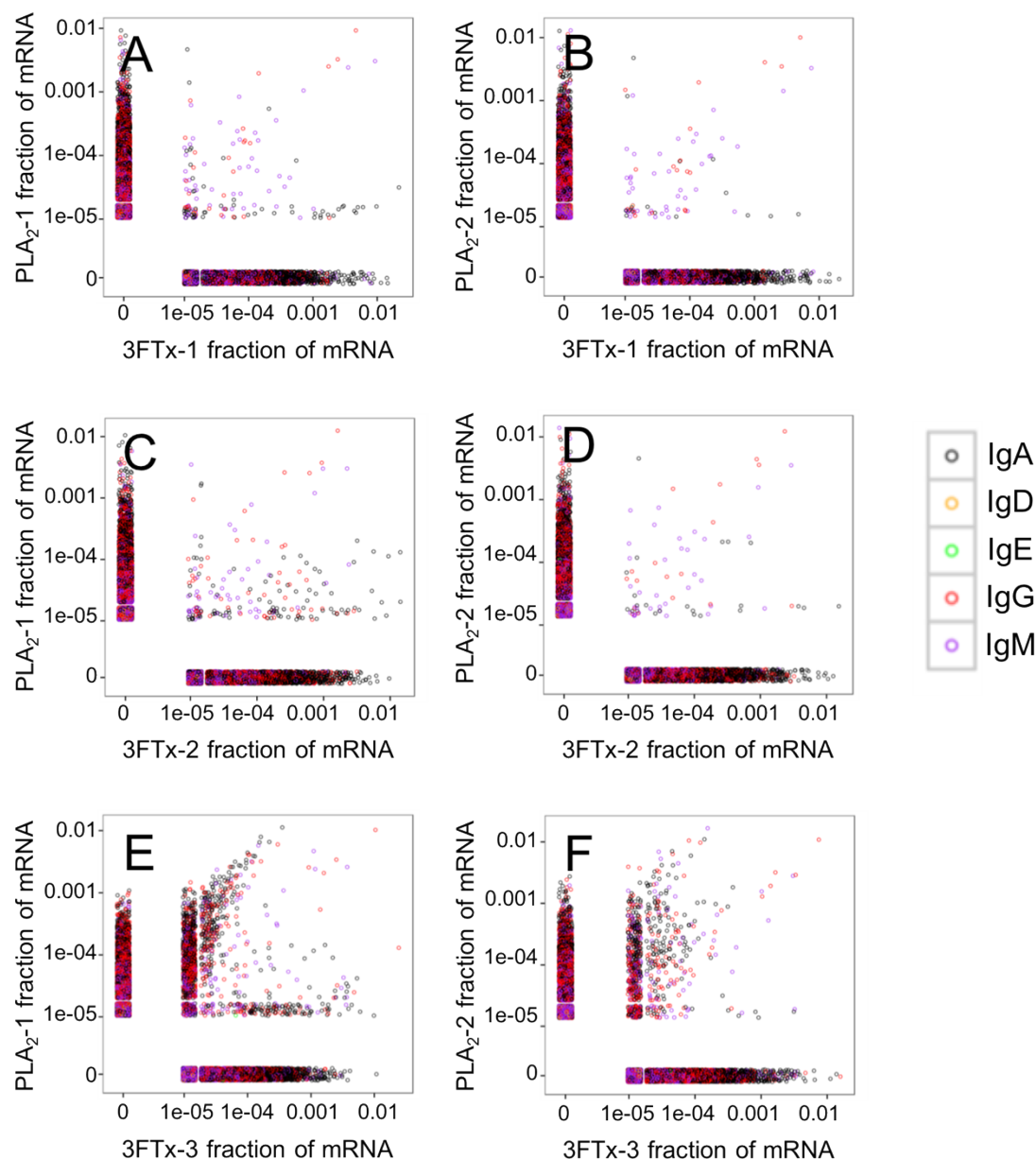
Figure 5: *Relative abundance of unique V_H clone transcripts compared between samples. Only few V_H transcripts are found in similar abundance in more than one mouse, when mice immunized with different toxins are compared.* **A)** *Comparison between mouse PLA$_2$-1 and 3FTx-1,* **B)** *Comparison between mouse PLA$_2$-2 and 3FTx-1,* **C)** *Comparison between mouse PLA$_2$-1 and 3FTx-2,* **D)** *Comparison between mouse PLA$_2$-2 and 3FTx-2,* **E)** *Comparison between mouse PLA$_2$-1 and 3FTx-3,* **F)** *Comparison between mouse PLA$_2$-2 and 3FTx-3.*

301

302   The AbSeq™ antibody sequencing methodology is capable of determining the Ig isotype of the

303   identified V_H clones. The coloring of the V_H clones in Fig. 4 and Fig. 5 reveals that a large

304   number of the most abundant V_H clones present in the mice are of the IgA isotype, which was

305   confirmed by further investigation of all mRNA transcripts from the splenocytes (Fig. 6). This is

306   surprising, as IgG is known to be the dominant immunoglobulin class in mouse blood after the

307   response to T-dependent protein antigens. The observation could possibly be explained by

308   differences in expression levels due to different translation rates and half-lives of mRNA

309   transcripts encoding different immunoglobulin isotypes. All approved antibody-based therapies

310   on the market are based on IgGs (*Walsh, 2014*), which are also the desired isotype for

311   antivenoms. In immunized horses for antivenom production, two isotypes of IgG are largely

312   responsible for the neutralization of toxic effects in the case of viperid snake venoms (*Fernandes*

313   *et al., 2000*). However, analysis of the transcripts obtained from the immunized mice revealed

314   only a low percentage of IgG transcripts, as compared to the transcripts for other Igs (Figs. 4-6).

315   With the acknowledgement of the small sample size employed in this study, this finding may

316   indicate a difficulty in raising potent IgG antibodies against both 3FTxs and PLA_2s in rodents. If

317   similar difficulty is present in horses, this may therefore have implications for antivenom

318   production. Our results may further suggest that the immune response is slightly lower against

319   3FTxs than for PLA_2s based on the lower abundance of IgG transcripts in mice immunized with

320   3FTx (Fig. 6). Taken together with the results from the ELISA assay (Fig. 2) and the observation

321   that immunization with PLA_2s is more prone to give rise to similar Ig transcripts (Fig. 4A vs.

322   Fig. 4B-D), we suggest that the PLA_2 toxins may possibly be slightly more immunogenic than

323   the 3FTx, although neither toxin seems to have high immunogenicity. The underlying reason for

324   this could possibly be due to the smaller molecular size of 3FTx compared to PLA_2s, or that

325   PLA_2s may contain distinct epitopes better capable of eliciting an adaptive immune response

326   than 3FTxs. Predictions of possible B-cell epitopes using the protein sequences and BepiPred 1.0

327   (*Larsen et al. 2006*) or DiscoTope 2.0 (*Kringelum et al. 2012*) with structural models of the

328   investigated toxins as input do not indicate a major difference in the bare number of possible

329   epitopes. However, the suggested difference in immunogenicity is further indicated by the fact

330   that only two IgG-encoding mRNA transcripts are found in the top 20 most abundant Ig-

331   encoding mRNA transcripts for only one out of three of the 3FTx-immunized mice. In

332   comparison, six and nine of the top 20 mRNA transcripts for mice immunized with PLA_2s

333   encode the IgG isotype (Fig. 7). It would be interesting to assess whether the immune response

334   of horses against these elapid venom toxins is also characterized by a low proportion of IgG − a

335   finding that would have evident implications for antivenom manufacture, as IgG has been shown

336   to be the antibody isotype of therapeutic value (*Fernandes et al., 2000*). However, this is beyond

337   the scope of this exploratory study.

338
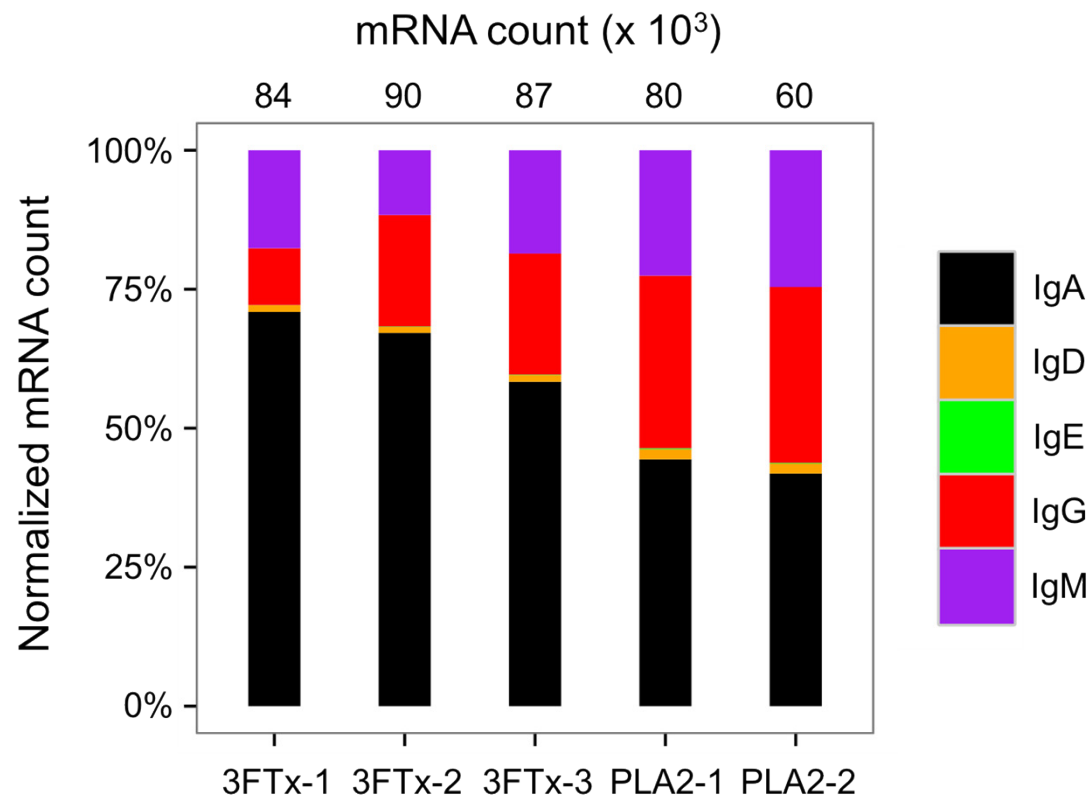
339

340 ***Figure 6:*** *Overview of total mRNA transcripts encoding different immunoglobulin isotypes from*

341 *the immunized mice (normalized). Numbers above each bar represents the mRNA count in each*

342 *sample.*

343

344
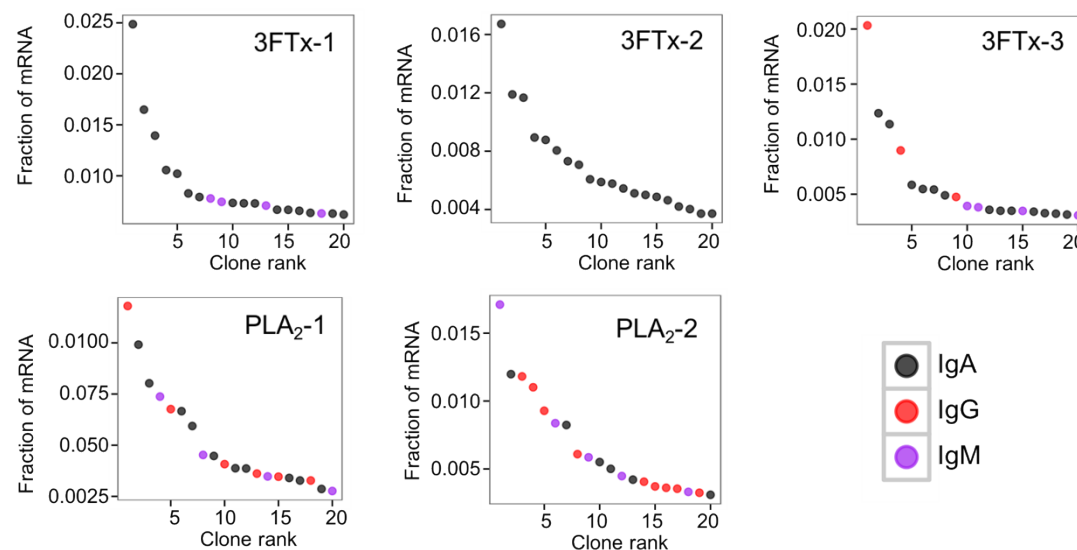
Figure 7: The 20 most abundant V_H clone transcripts and their corresponding isotypes in each

immunized mouse based on their fraction of total immunoglobulin mRNA.

347

4. Concluding remarks and outlook

349  In addition to demonstrating the utility of high-throughput sequencing technology,

350 AbSeq™, for investigation of immune responses in animals immunized with snake venom

351 toxins, the exploratory findings presented here may indicate possible difficulties in obtaining an

352 IgG response against the medically important toxins of the 3FTx and PLA_2 families from *M.*

353 *nigrocinctus*. Given that these proteins play key toxic roles in envenomings by elapid snakes, this

354 underlines a drawback of current antivenom production based on immunized animal serum, since

355 IgG has been shown to be the antibody isotype of therapeutic value (Fernandes et al., 2000).

356 Although based on a small exploratory sample size, these findings therefore contribute to the

357 understanding of snake toxin immunogenicity and indicate the possible difficulty in obtaining

358 balanced immune responses in animals during the immunization process.

359

360 **Acknowledgments**

361 We thank Mikael Rørdam Andersen from the Technical University of Denmark for

362 fruitful scientific discussion.

364   **References**

365   Alape-Girón A, Stiles B, Schmidt J, Girón-Cortés M, Thelestam M, Jörnvall H, Bergman T.

366   1996. Characterization of multiple nicotinic acetylcholine receptor-binding proteins and

367   phospholipases A_2 from the venom of the coral snake *Micrurus nigrocinctus nigrocinctus*.

368   *FEBS Letters* 380:29–32.

369   Antúnez J, Fernández J, Lomonte B, Angulo Y, Sanz L, Pérez A, Calvete JJ, Gutiérrez JM. 2010.

370   Antivenomics of *Atropoides mexicanus* and *Atropoides picadoi* snake venoms:

371   Relationship to the neutralization of toxic and enzymatic activities. *Journal of Venom*

372   *Research* 1:8–17.

373   Bolaños R, Cerdas L, Abalos JW. 1978. Venoms of coral snakes (*Micrurus* spp.): Report on a

374   multivalent antivenin for the Americas. *Bulletin of the Pan American Health Organization*

375   12:23–27.

376   Bolaños-Herrera R. 1972. Toxicity of Costa Rican snake venoms for the white mouse. *The*

377   *American Journal of Tropical Medicine and Hygiene* 21:360–363.

378   Bucaretchi F, De Capitani EM, Vieira RJ, Rodrigues CK, Zannin M, Da Silva Jr. NJ, Casais-e-

379   Silva LL, Hyslop S. 2016. Coral snake bites (*Micrurus* spp.) in Brazil: A review of

380   literature reports. *Clinical Toxicology* 54:222–234.

381   Campbell JA, Lamar WW. 2004. *The Venomous Reptiles of the Western Hemisphere. Vol. II.*

382   Ithaca, New York: Comstock Publishing Associates, Cornell University Press.

383   Castro KL, Duarte CG, Ramos HR, de Avila RAM, Schneider FS, Oliveira D, Freitas CF,

384   Kalapothakis E, Ho PL, Chávez-Olortegui C. 2015. Identification and characterization of

385   B-cell epitopes of 3FTx and PLA_2 toxins from *Micrurus corallinus* snake venom. *Toxicon*

386   93:51–60.

387   Chacón D, Arias J, Solano G, Bonilla F, Gómez A. 2012. Maintaining Coral Snakes (*Micrurus*

388   *nigrocinctus*, Serpentes: Elapidae) for venom production on an alternative fish-based diet.

389   *Toxicon* 60:249–253.

390   Chotwiwatthanakun C, Ronachai P, Akesowan S, Sriprapat S, Ratanabanangkoon K. 2001.

391   Production of potent polyvalent antivenom against three elapid venoms using a low dose,

392   low volume, multi-site immunization protocol. *Toxicon* 39:1487–1494.

393   Cook DAN, Owen T, Wagstaff SC, Kinne J, Wernery U, Harrison RA. 2010. Analysis of

394   camelid IgG for antivenom development: serological responses of venom-immunised

395   camels to prepare either monospecific or polyspecific antivenoms for West Africa. *Toxicon*

396   56:363–372.

397   Corrêa-Netto C, Junqueira-de-Azevedo IL, Silva DA, Ho PL, Leitão-de-Araújo M, Alves ML,

398   Sanz L, Foguel D, Zingali RB, Calvete JJ. 2011. Snake venomics and venom gland

399   transcriptomic analysis of Brazilian coral snakes, *Micrurus altirostris* and *M. corallinus*.

400   *Journal of Proteomics* 74:1795–1809.

401   Di Niro R, Lee SJ, Vander Heiden JA, Elsner RA, Trivedi N, Bannock JM, Gupta NT, Kleinstein

402   SH, Vigneault F, Gilbert TJ, Meffre E. 2015. *Salmonella* infection drives promiscuous B

403   cell activation followed by extrafollicular affinity maturation. *Immunity* 43:120–131.

404   Edgar RC. 2004. MUSCLE: multiple sequence alignment with high accuracy and high

405   throughput. *Nucleic Acids Research* 32:1792–1797.

406   Fernández J, Alape-Girón A, Angulo Y, Sanz L, Gutiérrez JM, Calvete JJ, Lomonte B. 2011.

407   Venomic and antivenomic analyses of the Central American coral snake, *Micrurus*

408   *nigrocinctus* (Elapidae). *Journal of Proteome Research* 10:1816–1827.

409 Fernandes I, Lima EX, Takehara HA, Moura-da-Silva AM, Tanjoni I, Gutiérrez JM. 2000. Horse

410   IgG isotypes and cross-neutralization of two snake antivenoms produced in Brazil and

411   Costa Rica. *Toxicon* 38:633–44.

412 Fernández J, Vargas N, Pla D, Sasa M, Rey-Suárez P, Sanz L, Gutiérrez JM, Calvete JJ,

413   Lomonte B. 2015. Snake venomics of *Micrurus alleni* and *Micrurus mosquitensis* from the

414   Caribbean region of Costa Rica reveals two divergent compositional patterns in New

415   World elapids. *Toxicon* 107:217–233.

416 Guidolin RG, Marcelino RM, Gondo HH, Morais JF, Ferreira RA, Silva CL, Kipnis TL, Silva

417   JA, Fafetine J, da Silva WD. 2010. Polyvalent horse F(ab')$_2$ snake antivenom: development

418   of process to produce polyvalent horse F(ab')$_2$ antibodies anti-african snake venom. *African*

419   *Journal of Biotechnology* 9:2446–2455.

420 Gutiérrez JM, Lomonte B, Aird SD, da Silva Jr. NJ, 2016. Mecanismo de açao dos venenos de

421   cobras corais. In: As Cobras Corais do Brasil: Biologia, Taxonomia, Venenos e

422   Envenenamientos (da Silva Jr, N.J., Ed.), 415 pp. Editora PUC Goiás, GO, Brazil.

423 Gutiérrez JM, León G, Lomonte B, Angulo Y. 2011. Antivenoms for snakebite envenomings.

424   *Inflammation & Allergy Drug Targets* 10:369–380.

425 Gutiérrez JM, Sanz L, Flores-Díaz M, Figueroa L, Madrigal M, Herrera M, Villalta M, León G,

426   Estrada R, Borges A, Alape-Girón A, Calvete JJ. 2009. Impact of regional variation in

427   *Bothrops asper* venom on the design of antivenoms: Integrating antivenomics and

428   neutralization approaches. *Journal of Proteome Research* 9:564–577.

429 Judge RK, Henry PJ, Mirtschin P, Jelinek G, Wilce JA. 2006. Toxins not neutralized by brown

430   snake antivenom. *Toxicology and Applied Pharmacology* 213:117–125.

431 Kringelum JV, Lundegaard C, Lund O, Nielsen M. 2012. Reliable B cell epitope predictions:

432 impacts of method development and improved benchmarking. *PLoS Computational Biology*

433 8:e1002829.

434 Larsen JE, Lund O, Nielsen M. 2006. Improved method for predicting linear B-cell epitopes.

435 *Immunome Research* 2:1.

436 Laustsen AH, Lomonte B, Lohse B, Fernández J, Gutiérrez JM. 2015. Unveiling the nature of

437 black mamba (*Dendroaspis polylepis*) venom through venomics and antivenom

438 immunoprofiling: identification of key toxin targets for antivenom development. *Journal of*

439 *Proteomics* 119:126–142.

440 Laustsen AH, Engmark M, Milbo C, Johannesen J, Lomonte B, Gutiérrez JM, Lohse B. 2016.

441 From Fangs to Pharmacology: The Future of Snakebite Envenoming Therapy. *Current*

442 *Pharmaceutical Design* 22: 5270–5293.

443 Laustsen AH, Solà M, Jappe EC, Oscoz S, Lauridsen LP, Engmark M. 2016. Biotechnological

444 trends in spider and scorpion antivenom development. *Toxins* 8:1–33.

445 Leong PK, Fung SY, Tan CH, Sim SM, Tan NH. 2015. Immunological cross-reactivity and

446 neutralization of the principal toxins of *Naja sumatrana* and related cobra venoms by a

447 Thai polyvalent antivenom (Neuro Polyvalent Snake Antivenom). *Acta Tropica* 149:86–93.

448 Lomonte B, Sasa M, Rey-Suárez P, Bryan W, Gutiérrez JM. 2016a. Venom of the coral snake

449 *Micrurus clarki*: proteomic profile, toxicity, immunological cross-neutralization, and

450 characterization of a three-finger toxin. *Toxins* 8:138.

451 Lomonte B, Rey-Suárez P, Fernández J, Sasa M, Pla D, Vargas N, Bénard-Valle M, Sanz L,

452 Corrêa-Netto C, Núñez V, Alape-Girón A, Alagón A, Gutiérrez JM, Calvete JJ, 2016b.

453 Venoms of *Micrurus* coral snakes: evolutionary trends in compositional patterns emerging

454 from proteomic analyses. *Toxicon* (submitted).

455 Mardis ER. 2008. Next-generation DNA sequencing methods. *Annual Review of Genomics and*
456   *Human Genetics* 9:387–402.

457 Nielsen M, Lundegaard C, Lund O, Petersen TN. 2010. CPHmodels-3.0—remote homology
458   modeling using structure-guided sequence profiles. *Nucleic Acids Research* gkq535.

459 Ownby C, Colberg T. 1990. Comparison of the immunogenicity and antigenic composition of
460   several venoms of snakes in the family Crotalidae. *Toxicon* 1990 28:189–199.

461 R Core Team (2014). R: A language and environment for statistical computing. R Foundation for
462   Statistical Computing, Vienna, Austria. URL http://www.R-project.org/.

463 Ramos HR, Junqueira-de-Azevedo ILM, Novo JB, Castro K, Duarte CG, Machado-de-Avila RA,
464   Chavez-Olortegui C, Ho PL. 2016. A heterologous multiepitope DNA prime/recombinant
465   protein boost immunisation strategy for the development of an antiserum against *Micrurus*
466   *corallinus* (coral snake) venom. *PLoS Neglected Tropical Diseases* 10:e0004484.

467 Rey-Suárez P, Núñez V, Gutiérrez JM, Lomonte B. 2011. Proteomic and biological
468   characterization of the venom of the redtail coral snake, *Micrurus mipartitus* (Elapidae),
469   from Colombia and Costa Rica. *Journal of Proteomics* 75:655–667.

470 Rey-Suárez P, Stuani-Floriano R, Rostelato-Ferreira S, Saldarriaga M, Núñez V, Rodrigues-
471   Simioni L, Lomonte B. 2012. Mipartoxin-I, a novel three-finger toxin, is the major
472   neurotoxic component in the venom of the redtail coral snake *Micrurus mipartitus*
473   (Elapidae). *Toxicon* 60:851–863.

474 Rey-Suárez P, Núñez V, Fernández J, Lomonte B. 2016. Integrative characterization of the
475   venom of the coral snake *Micrurus dumerilii* (Elapidae) from Colombia: proteome,
476   toxicity, and cross-neutralization by antivenom. *Journal of Proteomics* 136:262–273.

477   Rosso JP, Vargas-Rosso O, Gutiérrez JM, Rochat H, Bougis PE. 1996. Characterization of α-

478   neurotoxin and phospholipase A_2 activities from *Micrurus* venoms. *European Journal of*

479   *Biochemistry* 238:231–239.

480   Sanz L, Pla D, Pérez A, Rodríguez Y, Zavaleta-Martínez A, Salas M, Lomonte B, Calvete JJ.

481   2016. Venomic analysis of the poorly studied desert coral snake, *Micrurus tschudii*

482   *tschudii*, supports the 3FTx/PLA_2 dichotomy across *Micrurus* venoms. *Toxins* 8:178.

483   Schottler WH. 1951. Antigen-antibody relations in the present antivenin production of Brazil.

484   *American Journal of Tropical Medicine and Hygiene* 31:500–509.

485   Stern JN, Yaari G, Vander Heiden JA, Church G, Donahue WF, Hintzen RQ, Huttner AJ, Laman

486   JD, Nagra RM, Nylander A, Pitt D. 2014. B cells populating the multiple sclerosis brain

487   mature in the draining cervical lymph nodes. *Science Translational Medicine* 6:248ra107.

488   Tan KY, Tan CH, Fung SY, Tan NH. 2016. Neutralization of the Principal Toxins from the

489   Venoms of Thai *Naja kaouthia* and Malaysian *Hydrophis schistosus*: Insights into Toxin-

490   Specific Neutralization by Two Different Antivenoms. *Toxins* 8:1–17.

491   Tan CH, Tan KY, Lim SE, Tan NH. 2015. Venomics of the beaked sea snake, *Hydrophis*

492   *schistosus*: A minimalist toxin arsenal and its cross-neutralization by heterologous

493   antivenoms. *Journal of Proteomics* 126:121–30.

494   Tanaka G, Furtado MFD, Portaro FCV, Sant'Anna OA, Tambourgi DV. 2010. Diversity of

495   *Micrurus* snake species related to their venom toxic effects and the prospective of

496   antivenom neutralization. *PLoS Neglected Tropical Diseases* 4:622.

497   Tanaka GD, Sant'Anna OA, Marcelino JR, da Luz ACL, da Rocha MMT, Tambourgi DV. 2016.

498   *Micrurus* snake species: venom immunogenicity, antiserum cross-reactivity and

499   neutralization potential. *Toxicon* 117:59–68.

500   Tsioris K, Gupta NT, Ogunniyi AO, Zimnisky RM, Qian F, Yao Y, Wang X, Stern JN, Chari R,

501   Briggs AW, Clouser CR. 2015. Neutralizing antibodies against West Nile virus identified

502   directly from human B cells by single-cell analysis and next generation sequencing.

503   *Integrative Biology* 7:1587–1597.

504   Vander Heiden JA, Yaari G, Uduman M, Stern JN, O'Connor KC, Hafler DA, Vigneault F,

505   Kleinstein SH. 2014. pRESTO: a toolkit for processing high-throughput sequencing raw

506   reads of lymphocyte receptor repertoires. *Bioinformatics* 30:1930–1932

507   Vergara I, Pedraza-Escalona M, Paniagua D, Restano-Cassulini R, Zamudio F, Batista CV,

508   Possani L., Alagón A. 2014. Eastern coral snake *Micrurus fulvius* venom toxicity in mice is

509   mainly determined by neurotoxic phospholipases A_2. *Journal of Proteomics* 105:295–306.

510   Walsh G. 2014. Biopharmaceutical benchmarks 2014. *Nature biotechnology* 32:992–1000.

511   Warrell DA. 2010. Snake bite. *Lancet* 375:77–88.

512   Warrell DA. 2004. Snakebites in Central and South America: Epidemiology, clinical features

513   and clinical management. In: Campbell JA, Lamar WW, Eds. *The Venomous Reptiles of the*

514   *Western Hemisphere. Vol. II*. Ithaca, New York: Comstock Publishing Associates, Cornell

515   University Press, 709–761.

516   Williams DJ, Gutiérrez JM, Calvete JJ, Wüster W, Ratanabanangkoon K, Paiva O, Brown NI,

517   Casewell NR, Harrison RA, Rowley PD, O'Shea M. 2011. Ending the drought: new

518   strategies for improving the flow of affordable, effective antivenom in Asia and Africa.

519   *Journal of Proteomics* 74:1735–1767.

520   Wong KY, Tan CH, Tan NH. 2016. Venom and purified toxins of the spectacled cobra (*Naja*

521   *naja*) from Pakistan: Insights into toxicity and antivenom neutralization. *The American*

522   *Journal of Tropical Medicine and Hygiene* 94:1392–1399.

523   Ye J, Ma N, Madden TL, Ostell JM. 2013. IgBLAST: an immunoglobulin variable domain

524   sequence analysis tool. *Nucleic Acids Research* 41:W34-W40.

525